Title:
Acceleration of Coupled Granular Flow and Fluid Flow Simulations in Pebble Bed Energy Systems

Author names and affiliations:
Yanheng Li
Department of Mechanical, Aerospace, and Nuclear Engineering
Rensselaer Polytechnic Institute
110 8th street
Troy, New York, USA
liy19@rpi.edu

Wei Ji* (Corresponding author)
Department of Mechanical, Aerospace, and Nuclear Engineering
Rensselaer Polytechnic Institute
110 8th street
Troy, New York, USA
Tel: 1-(518)2766602
Fax: 1-(518)2766025
jiw2@rpi.edu

ABSTRACT

Fast and accurate approaches to simulating the coupled particle flow and fluid flow are of importance to the analysis of large particle-fluid systems. This is especially needed when one tries to simulate pebble flow and coolant flow in Pebble Bed Reactor (PBR) energy systems on a routine basis. As one of the Generation IV designs, the PBR design is a promising nuclear energy system with high fuel performance and inherent safety. A typical PBR core can be modeled as a particle-fluid system with strong interactions among pebbles, coolants and reactor walls. In previous works, the coupled Discrete Element Method (DEM)-Computational Fluid Dynamics (CFD) approach has been investigated and applied to modeling PBR systems. However, the DEM-CFD approach is computationally expensive due to large amounts of pebbles in PBR systems. This greatly restricts the PBR analysis for the real time prediction and inclusion of more physics. In this work, based on the symmetry of the PBR geometry and the slow motion characteristics of the pebble flow, two acceleration strategies are proposed. First, a simplified 3D-DEM/2D-CFD approach is proposed to speed up the DEM-CFD simulation without loss of accuracy. Pebble flow is simulated by a full 3-D DEM, while the coolant flow field is calculated with a 2-D CFD simulation by averaging variables along the annular direction in the cylindrical

and annular geometries. Second, based on the slow motion of pebble flow, the impact of the coupling frequency on the computation accuracy and efficiency is investigated. It shows that the coupling frequency can be decreased to an optimal frequency without affecting the method fidelity. By analyzing one of the PBR systems, the HTR-10 design, we show that the combined acceleration strategies can reduce the simulation time by 80% while retaining the same accuracy as the tightly coupled 3-D DEM and 3-D CFD simulations. Therefore, it is expected that the proposed acceleration methods can advance the coupled DEM-CFD approach to analyze the PBR, accounting for more physics such as thermal and neutronic effects, on a routine basis.

Key Words: Particle-Fluid System, Pebble Bed Reactors, Discrete Element Method, Computational Fluid Dynamics, Multi-physics Coupling

1. INTRODUCTION

Particle-fluid systems can be found in many applications in the energy industry. Examples of these energy systems include fluidized-bed chemical reactors (Yates, 1983), fluidized-bed based combustion chambers (Lyngfelt et al., 2001) and high temperature gas-cooled pebble bed reactors (Teuchert and Rutten, 1975). As a promising candidate for the next generation nuclear energy systems, Pebble Bed Reactors (PBRs) offer superior advantages in terms of fuel efficiency and operation safety over other nuclear reactor systems (Teuchert and Rutten, 1975). These advantages are rooted in its unique fuel design: hundreds of thousands of fuel pebbles are constantly recirculating in an active reactor core region, producing high power heat. Meanwhile, gas or liquid coolants are driven at high pressure through the interstices of these fuel pebbles to take the fission heat for electricity generation. The stochastic motion and the random distribution of fuel pebbles present great challenges in the analysis of reactor physics and thermal-hydraulics for the PBR designs(Hao et al., 2012). Complicated pebble-pebble and pebble-coolant interactions make the prediction of fuel pebble distribution and coolant properties even more difficult because of strong coupling between the pebble flow and coolant flow (Li and Ji, 2011, 2013). A full understanding of the fuel and coolant behavior in PBRs is of importance to the assessment of the reactor core performance and the operation safety. This is especially prominent when one analyzes the PBR design under extreme conditions, such as an earthquake or loss of coolant accident. To obtain the realistic model that describes the behaviors of the fuel pebble and

coolant, a highly accurate and efficient method is needed to simulate both pebble and coolant flows in PBRs.

Many approaches have been developed to simulate coupled particle and fluid flows in particle-fluid systems. These approaches can be divided into three groups based on how each flow is treated: fluid-fluid model, particle-fluid model and particle-particle model. The typical fluid-fluid model is usually named as two-fluid model (Drew, 1983; Drew and Lahey, 1993; Enwald et al., 1996; Ishii, 1975). In this model, each flow is treated like a continuum fluid flow. For particle flow, particles are spatially homogenized. The kinetic motion of the homogenized particles is approximated by kinetic theory (Lun, 1991; Lun et al., 1984). For fluid flow, ensemble-averaged fluid dynamics equations are formulated based on the two-phase flow theory (Drew, 1983; Ishii, 1975). The particle-fluid system is treated as an interpenetrating mixture of two fluids (Ishii, 1975). The coupling between particle and fluid flows is realized by introducing an interaction term, which is usually obtained based on empirical correlations. Two-fluid models have good computation efficiency at the price of low fidelity. The kinetic theory used for particle flow is based on the binary particle collision assumption, which is quite effective for dilute particle flows. The assumption, however, becomes inaccurate for dense granular flows (Forterre and Pouliquen, 2008). In PBRs, pebble flow is a quasi-static dense flow. Two-fluid models become ineffective in simulating coupled pebble and coolant flows, especially in the region near the reactor wall where wall effects are significant (Rycroft et al., 2006). On the other hand, particle-particle models treat both flows as discrete particle flows and track the motion of each solid particle and fluid “particle” by Direct Numerical Simulation (DNS). No assumptions or empirical models are used, therefore this model has very high fidelity (Hu et al., 2001). However, the computational cost is extremely high so this model has limited applicability for large scale systems. Currently, the DNS can only handle a particle-fluid system consisting of up to a few thousand particles (Tsuji, 2007). It is impossible to use the DNS to analyze PBR designs, such as the PBMR-400 design with more than 400,000 pebbles within the active core (Reitsma, 2012). As a compromise between efficiency and accuracy, particle-fluid models are proposed for the coupled modeling of fluid-particle systems. In practice, the most widely used approach is the coupled Discrete Element Method (DEM)-Computational Fluid Dynamics (CFD) approach (Zhu et al., 2007). In the DEM-CFD approach, the DEM is used to simulate the particle flow,

accounting for all the essential particle contact physics(Cundall and Strack, 1979). Therefore, the DEM model can track each solid particle's location and velocity accurately. For the fluid flow, the CFD model is used to compute the cell-averaged fluid quantities. It is the local average of the fluid properties that expedites the overall efficiency compared with high fidelity particle-particle models. With a good balance between fidelity and efficiency, the DEM-CFD approach is the most popular and pragmatic method that is used in analyzing particle-fluid systems, such as a fluidized bed (Yates, 1983).

Although the DEM-CFD approach is a good choice for the fluid-particle system simulation, it is still too expensive for PBR applications. Taking detailed pebble contact mechanics and coolant fluid dynamics into account, the simulation of one circulation cycle of the pebble flow in a small scale PBR core, such as the HTR-10 design (Gao and Shi, 2002) which is a gas-cooled pebble bed reactor loaded with around 30,000 pebbles, requires more than one week of computation time on a Dell T7500 3.6GHz workstation (Li and Ji, 2013). It is even more challenging to further extend the application of the DEM-CFD approach to transient analyses. For example, in accidental scenarios such as earthquakes (Ougouag et al., 2009), fast decisions are crucial to mitigate the damage of the facility. At the current efficiency of the DEM-CFD simulation, however, it is impossible to conduct a real time analysis under accidental transient scenarios. Moreover, thermal effect and neutronic performance are two other major design factors of a PBR, which further necessitates the enhancement of the computation efficiency. Based on these motivations, it is desirable to accelerate the DEM-CFD simulation and make it work on a routine basis in practical applications. In this paper, two acceleration strategies are proposed for speeding up the coupled pebble flow and coolant flow simulation in PBRs.

First, a simplified 3D-DEM/2D-CFD approach is proposed. The pebble flow is simulated by a full 3D DEM model to capture all the solid contact physics. The coolant flow is simulated in a reduced 2D CFD model, where the fluid quantities are averaged over the tangential direction. In the reactor physics and thermal analyses of PBRs, the axial and radial distributions of the power density and thermal temperature in the core are the key quantities and primary concerns to the safety assessment. This is so for two reasons. One is that the cylindrical or annular PBR core designs are axisymmetric. The other is that the dominant driving forces on the pebble flow and

coolant flow are along the axial and radial directions in PBR designs (Toit et al., 2006). All these factors, whether the geometric symmetry or the actual pebble/coolant flow driving force characters, result in an insignificant tangential flow component that is not of key interest to PBR analysts. Therefore, the tangential coolant flow component can be smeared out in the 3D Navier-Stokes equations and reduce the CFD computational load significantly.

Second, in addition to the dimension reduction in CFD calculations, the coupling frequency between the pebble flow and coolant flow simulations can also be relaxed to increase the efficiency. The coupling frequency is a measure of how often the DEM and CFD simulations exchange information for each flow simulation. Since the DEM time step length Δt_{DEM} is determined by the graphite pebble material properties and is usually restricted within a small range, this value is fixed in current work for convenience. Therefore we can use the inverse of Δt_{DEM} (denoted by ω_0) as the unit of coupling frequency. The coupling frequency of $0.01\omega_0$ adopted by previous work (Li and Ji, 2013) (1 CFD calculation per 100 DEM time steps) was originally designed for a fast moving fluidized bed (Kafui et al., 2002; Xiao and Sun, 2011). In PBRs, however, the pebble flow is almost static compared with coolant flow. The slow flow character can allow relaxing the tight coupling frequency to an interval during which the pebble packing statistics experience appreciable changes in a computational fluid cell. In this work, the impact of the coupling frequency on the accuracy and efficiency of PBR modeling is investigated. The optimal frequency is determined, which is on the order of $1e\text{-}6\omega_0$.

The remainder of the paper is organized as follows. The multi-physics model and the coupling framework used in the DEM-CFD simulation for particle-fluid systems are introduced in Section 2. Section 3 introduces the two acceleration approaches, each followed by detailed numerical simulation demonstration and justification in terms of accuracy and efficiency. An HTR-10 PBR design is employed as the study case. Finally, we close with a summary of our conclusions in Section 4.

2. MULTI-PHYSICS MODELING AND SIMULATION OF PEBBLE-COOLANT SYSTEMS

In this section, we introduce the multi-physical model that is used for the simulation of

pebble-coolant energy systems based on the coupled DEM-CFD methodology. The motion of each pebble is tracked by the discrete particle equation of motion and rotation at fine time steps, in which all the inter-pebble and pebble-wall contact is accounted for. For the simulation of coolant fluid dynamics, fluid-cell averaged mass and momentum conservation equations are used to address the spatial and temporal variation of coolant fluid quantities in a large scale energy system. Pebble packing statistics are explicitly accounted for in each fluid cell. Pebble flow and coolant flow are simulated based on the above dynamic equations and are closely coupled by the pebble-coolant interaction force. This interaction force is updated and exchanged between the pebble flow solver and the coolant flow solver at a reasonable frequency.

2.1. Governing Equations for Pebble Motion

The equations of motion for the pebbles are:

$$m\frac{d\mathbf{v}_\mathrm{i}}{dt} = \boldsymbol{F}_\mathrm{i} = \sum_{\substack{j\neq i \\ j=1}}^{N} \boldsymbol{F}_\mathrm{ij} + \boldsymbol{W}_\mathrm{i} + m_\mathrm{i}\boldsymbol{g} + \boldsymbol{F}_\mathrm{f,i}\,, \tag{1}$$

$$J_\mathrm{i}\frac{d\boldsymbol{\omega}_\mathrm{i}}{dt} = \boldsymbol{T}_\mathrm{i}\,, \tag{2}$$

where $\mathbf{v}_\mathrm{i}$ is the velocity of the *i*th pebble, $\boldsymbol{F}_\mathrm{i}$ is the net force on the *i*th pebble including $\boldsymbol{F}_\mathrm{ij}$ the contact force from the *j*th pebble, $\boldsymbol{W}_\mathrm{i}$ the wall contact force, $m_\mathrm{i}\boldsymbol{g}$ the gravitational force, and $\boldsymbol{F}_\mathrm{f,i}$ the fluid force. $\boldsymbol{T}_\mathrm{i}$ is the torque on *i*th pebble due to the tangential components of contact forces, $\boldsymbol{J}_\mathrm{i}$ is the momentum of inertial and $\boldsymbol{\omega}_\mathrm{i}$ is the angular velocity.

The pebble-to-pebble contact force $\boldsymbol{F}_\mathrm{ij}$ is composed of normal contact force $\boldsymbol{F}_\mathrm{n,ij}$ and tangential contact force $\boldsymbol{F}_\mathrm{t,ij}$, which can be evaluated based on Hertzian contact mechanics (Johnson, 1985).

The fluid-to-pebble force $\boldsymbol{F}_\mathrm{f,i}$ represents the forces that are exerted on the pebble from the fluid. In the case of dense and slow moving granular flow, the major interaction force is the drag force and pressure gradient force, which can be expressed as:

$$\boldsymbol{F}_\mathrm{f,i} = \boldsymbol{F}_\mathrm{D} + \boldsymbol{F}_\mathrm{P}\,, \tag{3}$$

$$\boldsymbol{F}_{\mathrm{D}} = \frac{1}{2}\rho(\boldsymbol{u}-\boldsymbol{u}_{\mathrm{P}})\left\|\boldsymbol{u}-\boldsymbol{u}_{\mathrm{P}}\right\| C_d \pi r^2 \alpha(\varepsilon)\,, \tag{4}$$

$$\boldsymbol{F}_{\mathrm{P}} = -\int_{V_{\mathrm{P}}} \nabla p dV\,, \tag{5}$$

where $\boldsymbol{F}_{\mathrm{D}}$ is the De Felice drag force (Di Felice, 1994), $\boldsymbol{F}_{\mathrm{P}}$ is the pressure gradient force, $\boldsymbol{u}$ is the fluid velocity, p is the pressure, ρ is the coolant density, $\boldsymbol{u}_{\mathrm{P}}$ is the pebble velocity, V_{P} is the volume of a pebble, ε is the local porosity, C_{d} is the drag coefficient, and $\alpha(\varepsilon)$ is an empirical function determined by ε and the Reynolds number Re (Di Felice, 1994).

2.2. Governing Equations for Fluid Motion and the Coupling Scheme

For a standard CFD model, the numerical solution for incompressible locally averaged Navier-Stokes (N-S) equations is needed. The 3-D N-S equations for the fluid phase in a cylindrical coordinate system are (Ekambara et al., 2005) (assuming constant coolant density):

$$\frac{\partial(\varepsilon)}{\partial t} + \frac{1}{r}\frac{\partial(\varepsilon r u_r)}{\partial r} + \frac{1}{r}\frac{\partial(\varepsilon u_\theta)}{\partial \theta} + \frac{\partial(\varepsilon u_z)}{\partial z} = 0 \tag{6}$$

$$\begin{aligned}\rho_f[\frac{\partial(\varepsilon u_r)}{\partial t} + u_r\frac{\partial(\varepsilon u_r)}{\partial r} + \frac{u_\theta}{r}\frac{\partial(\varepsilon u_r)}{\partial \theta} + u_z\frac{\partial(\varepsilon u_r)}{\partial z} - \frac{u_\theta^{\,2}}{r}] = -\varepsilon\frac{\partial p}{\partial r} + \\ \mu_f\{\frac{1}{r}\frac{\partial}{\partial r}[r\frac{\partial(\varepsilon u_r)}{\partial r}] + \frac{1}{r^2}\frac{\partial^2(\varepsilon u_r)}{\partial \theta^2} + \frac{\partial^2(\varepsilon u_r)}{\partial z^2} - \frac{\varepsilon u_r}{r^2} - \frac{2}{r^2}\frac{\partial(\varepsilon u_\theta)}{\partial \theta}\} + f_{pr},\end{aligned} \tag{7}$$

$$\begin{aligned}\rho_f[\frac{\partial(\varepsilon u_z)}{\partial t} + u_r\frac{\partial(\varepsilon u_z)}{\partial r} + \frac{u_\theta}{r}\frac{\partial(\varepsilon u_z)}{\partial \theta} + u_z\frac{\partial(\varepsilon u_z)}{\partial z}] = -\varepsilon\frac{\partial p}{\partial z} + \\ \mu_f\{\frac{1}{r}\frac{\partial}{\partial r}[r\frac{\partial(\varepsilon u_z)}{\partial r}] + \frac{1}{r^2}\frac{\partial^2(\varepsilon u_z)}{\partial \theta^2} + \frac{\partial^2(\varepsilon u_z)}{\partial z^2}\} + f_{pz} + \varepsilon\rho_f g,\end{aligned} \tag{8}$$

$$\begin{aligned}\rho_f[\frac{\partial(\varepsilon u_\theta)}{\partial t} + u_r\frac{\partial(\varepsilon u_\theta)}{\partial r} + \frac{u_\theta}{r}\frac{\partial(\varepsilon u_\theta)}{\partial \theta} + u_z\frac{\partial(\varepsilon u_\theta)}{\partial z} + \frac{u_\theta u_r}{r}] = -\varepsilon\frac{1}{r}\frac{\partial p}{\partial \theta} + \\ \mu_f\{\frac{1}{r}\frac{\partial}{\partial r}[r\frac{\partial(\varepsilon u_\theta)}{\partial r}] + \frac{1}{r^2}\frac{\partial^2(\varepsilon u_\theta)}{\partial \theta^2} + \frac{\partial^2(\varepsilon u_\theta)}{\partial z^2} + \frac{2}{r^2}\frac{\partial(\varepsilon u_r)}{\partial \theta} - \frac{\varepsilon u_\theta}{r^2}\} + f_{p\theta},\end{aligned} \tag{9}$$

where ε is the average porosity in a fluid cell, ρ_f is the average fluid density in a fluid cell, μ_f is the fluid dynamic viscosity, u is the average fluid velocity in a fluid cell, and p is the average fluid pressure. f_{pr}, f_{pz} and $f_{\mathrm{p\theta}}$ are the radial, axial and tangential components of the total force

density $\boldsymbol{f}_{\mathrm{p}}$ that is exerted on the fluid by all the pebbles that fall into the fluid cell.

In order to solve Eqs. (6)-(9), the reactor core is divided into three dimensional cells first in the cylindrical coordinate system. The average porosity in each cell is calculated by accumulating the pebble volume within the cell. Then a semi-implicit finite difference method (Verzicco and Orlandi, 1996) is used to solve the incompressible N-S equations iteratively. In practice, a cell size of about a few particle diameters (3-5 times in this work) is adopted (Lim et al., 2006). It has been shown (Li and Ji, 2013) that such a size is 1) large enough in the sense that the fluid details are averaged within the cell and the relative position of particles and porosity calculation error does not have a noticeable impact on the averaged fluid quantities within a cell, and 2) local and small enough in the sense that the spatial variation of packing fraction within the overall geometry can still be represented, with the utilization of certain techniques for more accuracy, such as "particle-source-in-cell method"(Parry and Millet, 2010).

2.3. The Coupled DEM-CFD Framework

After obtaining the fluid-to-pebble force $\boldsymbol{F}_{\mathrm{f,i}}$, the pebble-to-fluid force density $\boldsymbol{f}_{\mathrm{p}}$, which is the force exerted onto a fluid cell from the pebbles within the fluid cell, can be calculated (Parry and Millet, 2010). The force density $\boldsymbol{f}_{\mathrm{p}}$ can be calculated by:

$$\boldsymbol{f}_{\mathrm{p}} = -\sum_{i}^{N_{\mathrm{c}}} \left[\beta_{\mathrm{i}} \sum (\boldsymbol{F}_{\mathrm{D}} + \boldsymbol{F}_{\mathrm{P}}) \right] \Big/ V_{\mathrm{cell}} \ , \tag{10}$$

where N_{c} is the number of pebbles within a fluid cell, V_{cell} is the volume of the fluid cell, and β_{i} is the volume fraction of i^{th} pebble that falls into the cell. The term $\boldsymbol{f}_{\mathrm{p}}$ is constant within each fluid cell and will be used in the fluid calculations.

A finite difference method with a staggered grid is used for CFD discretization. For each time step of CFD, the porosity and pebble velocities from the DEM calculation are used to calculate the drag force using Eq. (4). Since the DEM time step is much smaller than the CFD time step, the DEM solver and the CFD solver exchange data for every 100 DEM steps as the default coupling frequency, with porosity and fluid properties invariant between data exchanging. The schematics of 3D-DEM/3D-CFD is shown in Fig. 1, where $\boldsymbol{F}_{\mathrm{c}} = \boldsymbol{F}_n + \boldsymbol{F}_t$ is the pebble contact force.

From Fig. 1, it can be seen that the coupling between the particle phase and fluid phase is two way: either the particle phase or the fluid phase can transfer momentum through the particle-fluid interaction to the other phase and consequently have an impact on the field distribution of the other phase.

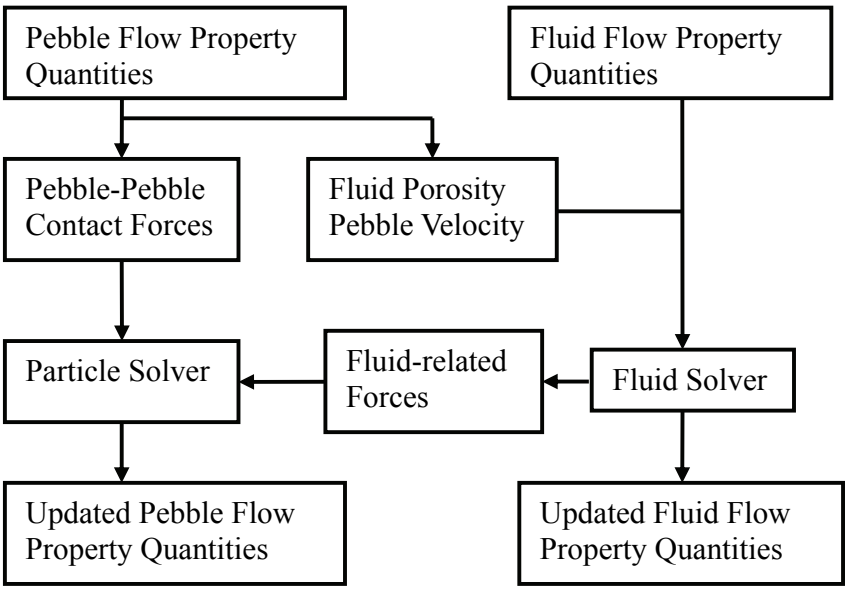

Figure 1. 3D-DEM/3D-CFD schematics

3. ACCELERATION OF THE COUPLED DEM-CFD ANALYSIS

Although a tightly coupled 3D DEM/3D CFD approach can preserve the physics well for coupled fluid-particle systems, it is computationally expensive. For example, to analyze a HTR-10 design which is a small scale PBR, it takes more than ten days to reach the steady state from the initial loading. For routine analysis, the acceleration method is desired to speed up existing coupled simulation framework. In this section, we will introduce two strategies. The first strategy is dimension reduction in the CFD model. This is due to the high computation demand in 3D CFD computation. As both the porosity calculation and the solution of the N-S equation in 3D requires a considerable amount of CPU time (For a 10 (radial) by 21 (axial) by 12 (tangential) meshing, it will take more than two minutes of computation on a Dell T7500 3.6GHz workstation without parallelization), and these calculations need to be performed at the designated coupling frequency, forming a major computational load in the overall multi-physics modeling simulation. In this strategy the fluid quantities are averaged over the tangential

directions and only axial and radial components are preserved. The second acceleration strategy is the relaxation of the coupling frequency. Previous tightly coupled schemes require the fluid quantities be updated for every 100 DEM steps. In reality, it may not be necessary due to the slow change of pebble flow character. Impact from different coupling frequencies onto the computation accuracy and efficiency are investigated to determine the optimal value.

For convenience and better illustration of the proposed acceleration strategies, two time constants are defined here. The first time constant is T_{cyl}, which is a measure of the period of the system and can be defined as the average time needed for a pebble to travel from the top to the bottom of the core at steady state. The other time constant is T_{inf}, which is the time needed from an initial loading condition to a steady state configuration and is mainly determined by the initial pebble configuration. These two time constants can be expressed either in realistic physical time or simulation CPU time. The simulation starts with the initialization of pebble packing generated by a newly developed sphere packing method (Li and Ji, 2012). The circulating process of the pebbles is realized through the adoption of periodic boundary conditions at the top and bottom surfaces. For every pebble, once its position is below the surface of the outlet, it will recur from the top of the core. This periodic boundary condition is close to the realistic operation case and can well preserve the total quantity and motion balance of the pebble flow.

In order to demonstrate the viability of both acceleration strategies, an HTR-10 application is investigated. The HTR-10 is a prototype pebble bed reactor (Gao and Shi, 2002). It has a cylindrical active core with a radius of 90cm and a height of 180cm, followed by a 45 degree conic bottom and a cylindrical chute. The pebbles are first loaded into the reactor from the top. The settling down of loaded pebbles in the core will result in a packed bed with packing fraction greater than 60% (Auwerda et al., 2010; Li and Ji, 2013; Rycroft et al., 2006). During the recirculation, pebbles are released from the bottom of the reactor through the chute, while new pebbles are inserted from the top of the reactor. Meanwhile, helium coolant is injected from the top of the reactor and emitted from the bottom of the reactor, with the boundary condition of constant velocity inlet and constant pressure outlet. The outside view of the reactor is shown as Fig. 2 (generated by Paraview), and the physical parameters for the pebble and coolant are listed in Table 1.1 and Table 1.2, respectively. The re-circulation is simulated until the system reaches a

steady state (at T_{inf}), which is slightly less than $0.5T_{cyl}$ for adopted initialization techniques. In order to better obtain pebble and coolant quantities at the steady state, such as the pebble packing statistics and velocity, the coolant velocity and pressure, the solutions presented in this paper are averaged over a short period (~5s) at the end of simulation time.

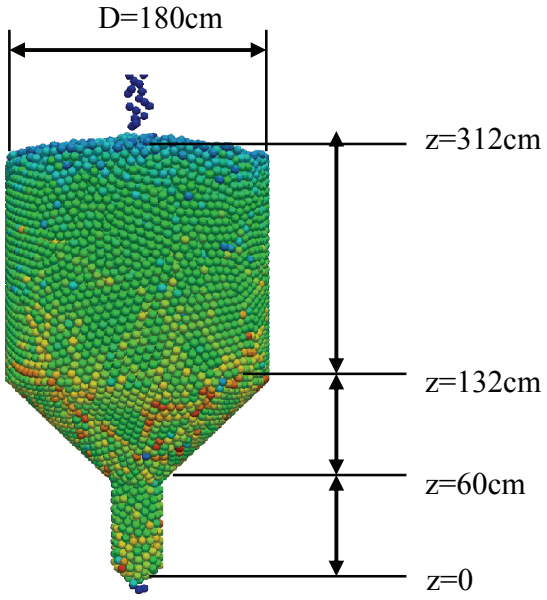

Figure 2. Reactor geometry and snapshot during pebble recirculation

Table 1.1. Pebble physical properties

Radius	Mass	Young's modulus	Friction coefficient	Poisson ratio
3 cm	210 g	1e9 Pa	0.7	0.3

Table 1.2. Helium coolant physical properties

Density	Dynamic viscosity	Specific heat	Mass flow rate	Outlet pressure
1.65 g/L	3.86e-5 Pa.s	5.19e3 J/Kg. K	4.32 kg/s	constant

Although the pebble motion has stochastic nature, a quasi-dynamic equilibrium state (steady state) exists, which represents the normal operation condition with near time-invariant spatial packing distributions of pebbles. Since the Pearson product-moment correlation coefficient (PCC) r_P has been employed widely to determine the correlation or similarity between two data sets (Häne et al., 1993; Rodgers and Nicewander, 1988), it is adopted in this work to quantitatively describe the steady state packing statistics for pebble flow. PCC for two data sets X and Y is defined as:

$$r_P = \frac{\mathrm{cov}(X,Y)}{\sigma_X \sigma_Y}, \tag{11}$$

where cov(X, Y) is the covariance of X and Y, and σ is the standard deviation. For a packing distribution $P(t)$ at time t, in order to determine whether it is a steady state packing, we can sample the packing distribution $P(t+\Delta t)$ after a time increment Δt (usually <10s for PBR application). Then the PCC between $P(t)$ and $P(t+\Delta t)$ can be computed. If r_P is very close to 1, it means that $P(t)$ and $P(t+\Delta t)$ are similar to each other (Rodgers and Nicewander, 1988). The radial and axial packing distributions of HTR-10 simulation at steady state (without time averaging) are shown as in Fig. 3a and Fig. 3b, respectively.

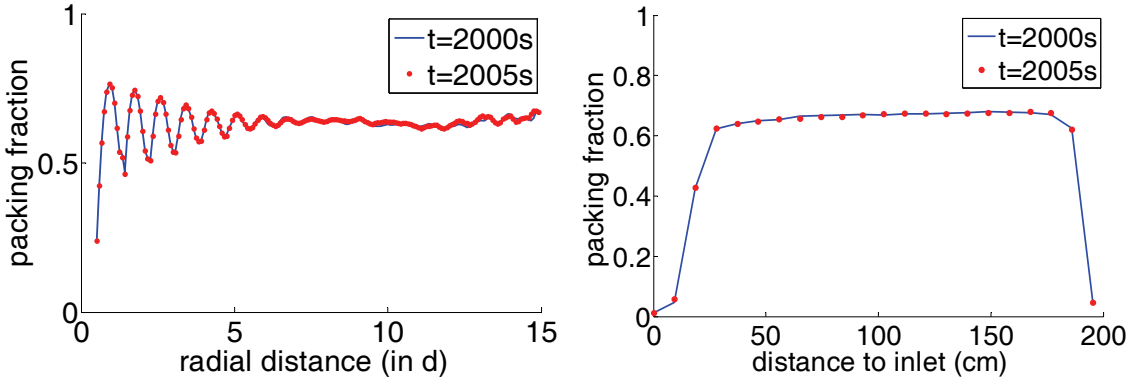

(a) radial packing fraction comparison (b) axial packing fraction comparison

Figure 3. Comparison of packing fraction distribution at steady state between two simulation times

It is obvious from Fig. 3 that the pebble flow is very close to the steady state because the packing statistics are almost time invariant. The PCC can quantify this similarity. For radial packing distribution P_r, and axial packing distribution P_a, based on Eq. (11), the PCC value between different times are calculated in Table 2, indicating a high similarity between two different packing statistics at steady state.

Table 2. Comparison of PCC value of packing distributions at different times

$r_P(P_r(2000s),P_r(2005s))$	$r_P(P_r(0s),P_r(2000s))$	$r_P(P_a(2000s),P_a(2005s))$	$r_P(P_a(0s),P_a(2000s))$
0.9932	0.9162	0.9998	0.9138

3.1 Dimension Reduction in Fluid-Phase Calculations

Axisymmetric core geometry exists in many energy systems, especially in nuclear energy systems. For a PBR system design, the reactor core is either cylindrical or annular. Moreover, the coolant and pebble flow are injected by forces along the axial direction or radial direction and are confined by the forces along the radial direction from the inner and outer walls. Such a highly axisymmetric geometry and dominant axial and radial flow driven forces would lead to a much smaller spatial variation of flow quantities along the tangential direction than that in the axial and radial direction. Therefore, it is common to average the fluid quantities over the tangential direction to obtain the simplified 2D fluid equations:

$$\frac{\partial(\varepsilon)}{\partial t}+\frac{1}{r}\frac{\partial(\varepsilon r u_r)}{\partial r}+\frac{\partial(\varepsilon u_z)}{\partial z}=0, \tag{12}$$

$$\rho_f\left[\frac{\partial(\varepsilon u_r)}{\partial t}+\frac{\partial(\varepsilon u_r u_r)}{\partial r}+\frac{\partial(\varepsilon u_z u_r)}{\partial z}\right]=-\varepsilon\frac{\partial p}{\partial r}+\mu_f\left\{\frac{1}{r}\frac{\partial}{\partial r}\left[r\frac{\partial(\varepsilon u_r)}{\partial r}\right]+\frac{\partial^2(\varepsilon u_r)}{\partial z^2}-\frac{\varepsilon u_r}{r^2}\right\}+\bar{f}_{pr}, \tag{13}$$

$$\rho_f\left[\frac{\partial(\varepsilon u_z)}{\partial t}+\frac{\partial(\varepsilon u_z u_r)}{\partial r}+\frac{\partial(\varepsilon u_z u_z)}{\partial z}\right]=-\varepsilon\frac{\partial p}{\partial z}+\mu_f\left\{\frac{1}{r}\frac{\partial}{\partial r}\left[r\frac{\partial(\varepsilon u_z)}{\partial r}\right]+\frac{\partial^2(\varepsilon u_z)}{\partial z^2}\right\}+\bar{f}_{pz}+\varepsilon\rho_f g, \tag{14}$$

where $\bar{f}_{pr}$ and $\bar{f}_{pz}$ are the radial and axial components of $\bar{\boldsymbol{f}}_p$ defined as $\bar{\boldsymbol{f}}_p=\frac{\int_0^{2\pi}\boldsymbol{f}_p d\theta}{2\pi}$.

From Eqs. (1)-(14), it can be seen that the two-way coupling in 3D-DEM/3D-CFD is still preserved in the simplified approach, and the only simplification is the averaging of fluid quantities over θ. By comparing Eqs. (6)-(9) and Eqs.(12)-(14), it can be seen that all the terms

containing u_θ and $\frac{\partial(.)}{\partial\theta}$ are dropped in the simplification process, and all the other quantities such as u_r, u_z, p, f_r and f_z are averaged over the tangential direction. Therefore, the fidelity loss during the simplification is determined by the magnitude of $\underline{u_\theta}$ and the tangential variation of all other averaged quantities.

A comparison between the full 3D simulation and the simplified 2D simulation is necessary to assure that the simplified approach does not result in much difference at the steady state with the full 3D simulation. As stated above, a fixed DEM time step of 1e-5s is adopted based on the graphite material properties which results in ω_0 =1e5s^{-1}, and a 0.01ω_0 coupling frequency is used as the default value in both calculations. Compared with full dimension computation, T_{inf} is reduced from 249 hours of CPU time to 72 hours in the simplified approach.

3.1.1 Steady-state pebble flow comparison

Pebble trajectory and packing statistics are important pebble flow quantities for PBR research. The dimension reduction in CFD calculations should not bring in large discrepancies in pebble trajectories. The PCC can also be adopted to determine the similarity between 2D and 3D results. The pebble trajectory comparison between 3D and 2D simulations starts with the same initial condition, then seven pebbles at approximately the same height but with different radial positions are chosen to be tracked, and the 3D trajectory is projected onto the r-z plane. The results are shown in Fig. 4a. Two neighboring points along a trajectory correspond with a time step of 100s. We can see that the pebble trajectories from the simplified approach will keep track with the full dimension computation results with the average PCC value of r_P=0.983. It can be seen that the dimension reduction will not cause significant change of T_{cyl}. As stated in the introduction, these similarities can be attributed to the facts that the HTR10 has axially symmetric geometry, axially oriented initial condition, and all the dominant forces are approximately aligned along the axial and radial direction, especially in the cylindrical core region.

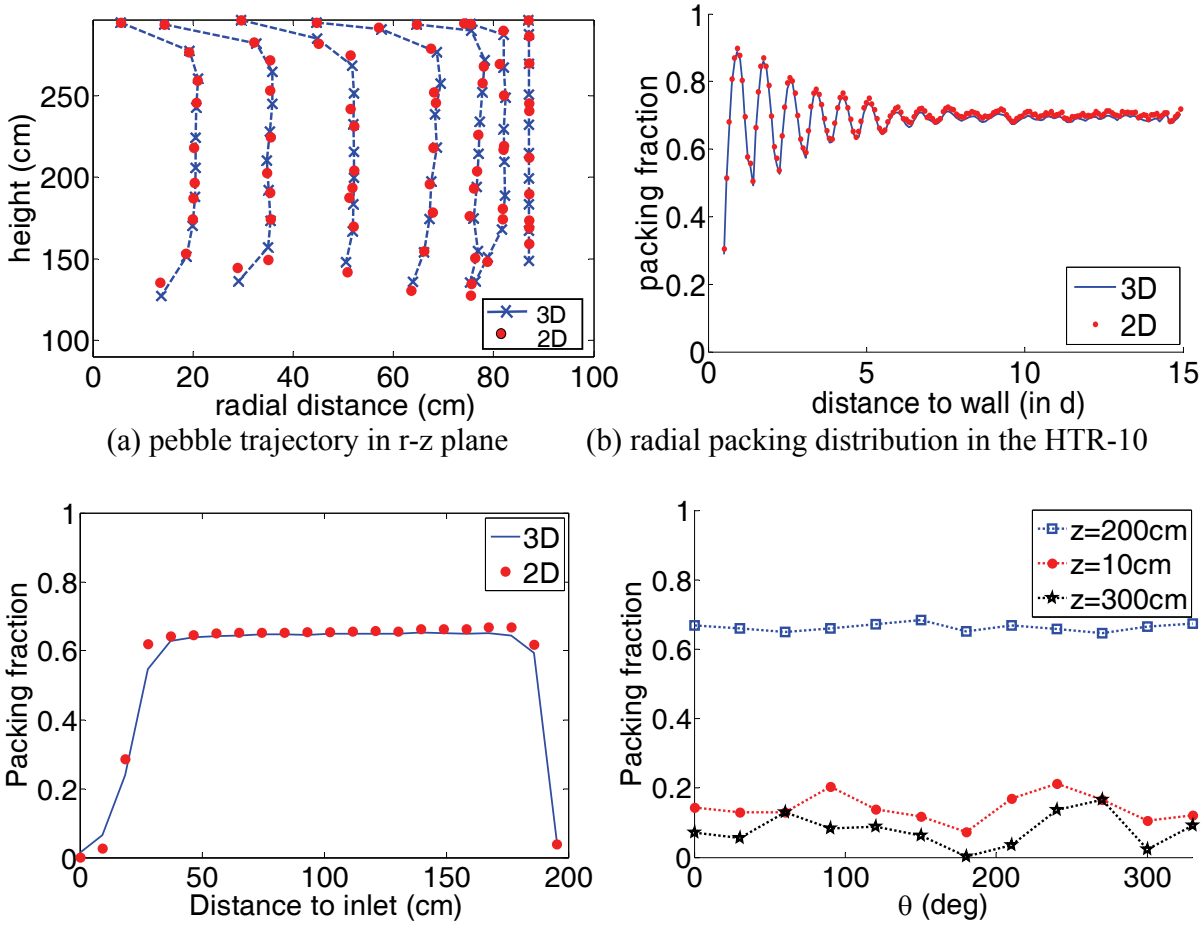

(a) pebble trajectory in r-z plane

(b) radial packing distribution in the HTR-10

(c) axial packing distribution

(d) tangential packing fraction distribution at different heights

Figure 4. Pebble flow comparison of pebble trajectory and packing distribution between 2D and 3D simulation

Besides the deterministic pebble trajectories, the spatial distributions of pebbles are also of key interest to neutronic and thermal analysts. To calculate the local packing fraction, the reactor core is meshed into cylindrical coordinate cells, and the volume of pebbles that falls into each cell is tallied. The local packing fraction can be determined by the ratio of the accumulated local pebble volume to the local cell volume. The radial and axial packing fraction at steady state for both 3D and 2D simulation are given in Fig. 4b and 4c, respectively. The PCC values for radial distributions between 3D and 2D CFD results are 0.989 and for axial distribution it is 0.994, indicating the reduction in dimension has an insignificant effect on the pebble packing. From the

axial packing statistics it can be seen that within the cylindrical core region the full dimension approach and simplified approach have a high similarity in axial packing fraction, while near the inlet and outlet region a slight difference is observed. To explain this difference, we refer to Eqs. (6)-(9). It can be seen that the local porosity has a direct influence on the fluid continuity and momentum conservation. And Fig.4c indicates that the pebble packing in these inlet/outlet regions are not as dense as that in the middle core region. Hence, the pebble contact forces are not as significant and the θ-component fluid-pebble interaction accounts for a greater portion among the overall external forces. In addition, the packing near the inlet/outlet region is not as even as that in the cylindrical core (Fig. 4d), therefore the tangential variation of pebble and fluid quantities is more significant which will cause further fidelity loss.

3.1.2 Steady-state fluid flow comparison

The average u_z and p variation along the axial direction is given, to prove that the 2D CFD approach can provide a very close pressure drop and the in-core axial fluid speed profile to the 3D simulations. The comparisons between 2D and 3D simulation solutions are shown in Fig. 5.

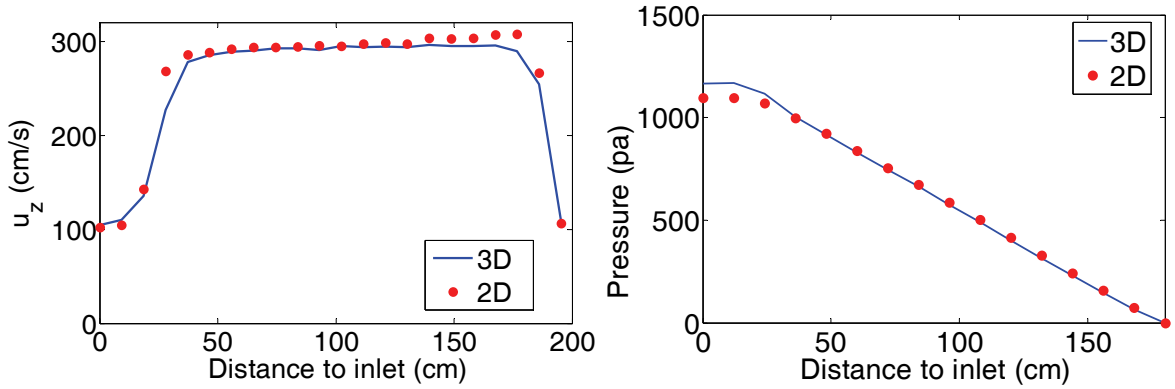

(a) radial distribution of u_z (b) pressure drop

Figure 5. Comparison of z-component coolant flow velocity and pressure drop between 2-D and 3-D simulations

From the axial profile of radially averaged u_z (Fig. 5a), it can be seen that the simplified approach slightly overestimates the magnitude of u_z in the bulk region and results in an underestimate of pressure drop. From the pressure drop curve (Fig. 5b) we can see that, the discrepancy of Δp between 3D and 2D simulation mainly occurs near the inlet region where the

annular motion of both pebble and fluid are more significant than in the bulk region. However, as indicated by Fig. 5a, the axial distributions of u_z throughout the core region from both 3D and 2D calculations do not show noticeable pattern difference except that the simplified result have slightly higher u_z magnitude which corresponds with the result from Fig.4c.

As seen in the formulation of $\overline{f}_p$, it can be realized that the fidelity of the simplified approach is determined by the magnitude of the θ-component force and variation of r-component and z-component force along the tangential direction. From the geometry aspect, a small variation of packing distribution along the θ-direction is crucial for the axial symmetry, which is verified in Fig. 6a. The u_z-θ profiles at R=25, 50 and 75cm (Fig. 6b) and the u_r-θ profiles at R=25, 50 and 75cm (Fig. 6c) suggests that the magnitude of $\frac{\partial u_z}{\partial \theta}\Big/u_z$ and $\frac{\partial u_r}{\partial \theta}\Big/u_r$ are very close to zero. The magnitude of u_θ is two orders less than that of u_z, as shown in Fig.6d. Moreover, the dominant force in the PBR application is the pebble contact force which is more than one order larger in magnitude than the fluid force Therefore the assumption during the simplification in this section is validated and this explains why the simplification has little impact on the pebble motion.

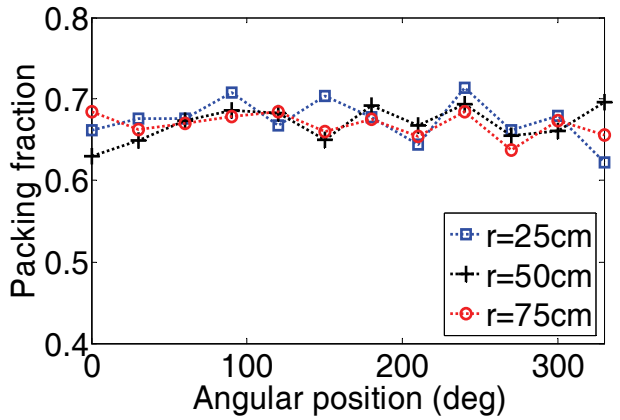

(a) tangential packing distribution

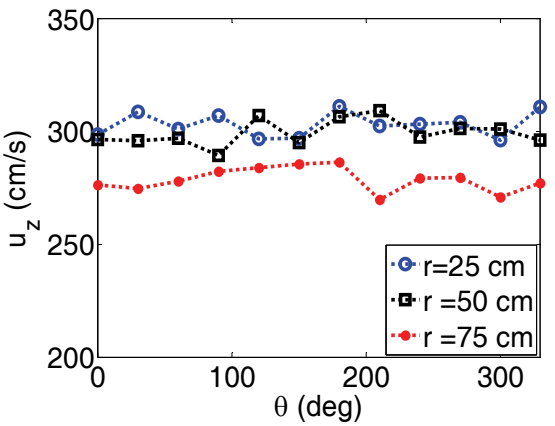

(b) u_z-θ profile

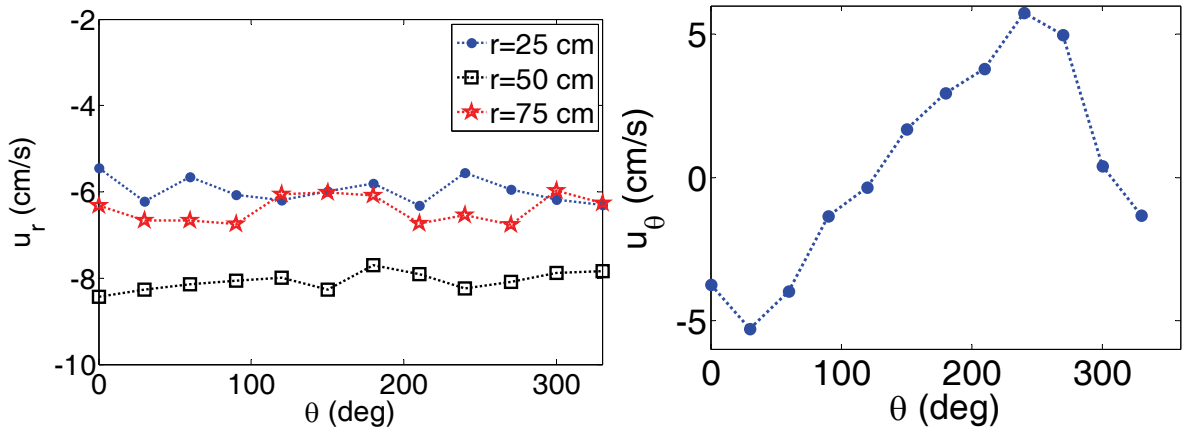

(c) u_r-θ profile (d) u_θ-θ profile at r=75cm

Figure 6. θ-component packing statistics and coolant flow comparison

3.2 Coupling Frequency Relaxation

As proposed by previous works (Li and Ji, 2013), the coupling frequency for the current result is based on a 1:100 of DEM to CFD ratio. This ratio can well preserve the fidelity within a wide range of applications, from slow moving particle sedimentation process to fast moving spout fluidized beds. For PBR applications, due to the relatively slow motion of pebbles compared with coolant flow (10^{-1} cm/s versus 10^{2} cm/s), the coupling frequency could be decreased in order to speed up the overall calculation. In order to find the optimal coupling frequency that provides the best balance between accuracy and efficiency, different coupling frequencies (denoted by ω) at one CFD calculation per 0.01s, 0.1s, 1s, 10s, 50s, 100s, 250s and 1000s, are employed to simulate the process from initial fuel loading to the steady state. First the frequency impact on calculation efficiency is investigated. Although the change of coupling frequency should not have a great impact on steady state constants T_{cyl}, it does have an impact on the transient time constants T_{inf}. Starting from the same initial condition, the CPU time to achieve the equilibrium steady state (T_{inf}) from different coupling frequencies is plotted in Fig. 7a, which shows that the best efficiency occurs from the frequency of 1e-6 ω_0 (1 CFD calculation per 10 second) to 1e-7ω_0 (1 CFD calculation per 10^2 seconds). It is worth noting that this "optimal" frequency corresponds with the time interval around (1e-2~1e-1)T_{inf}.

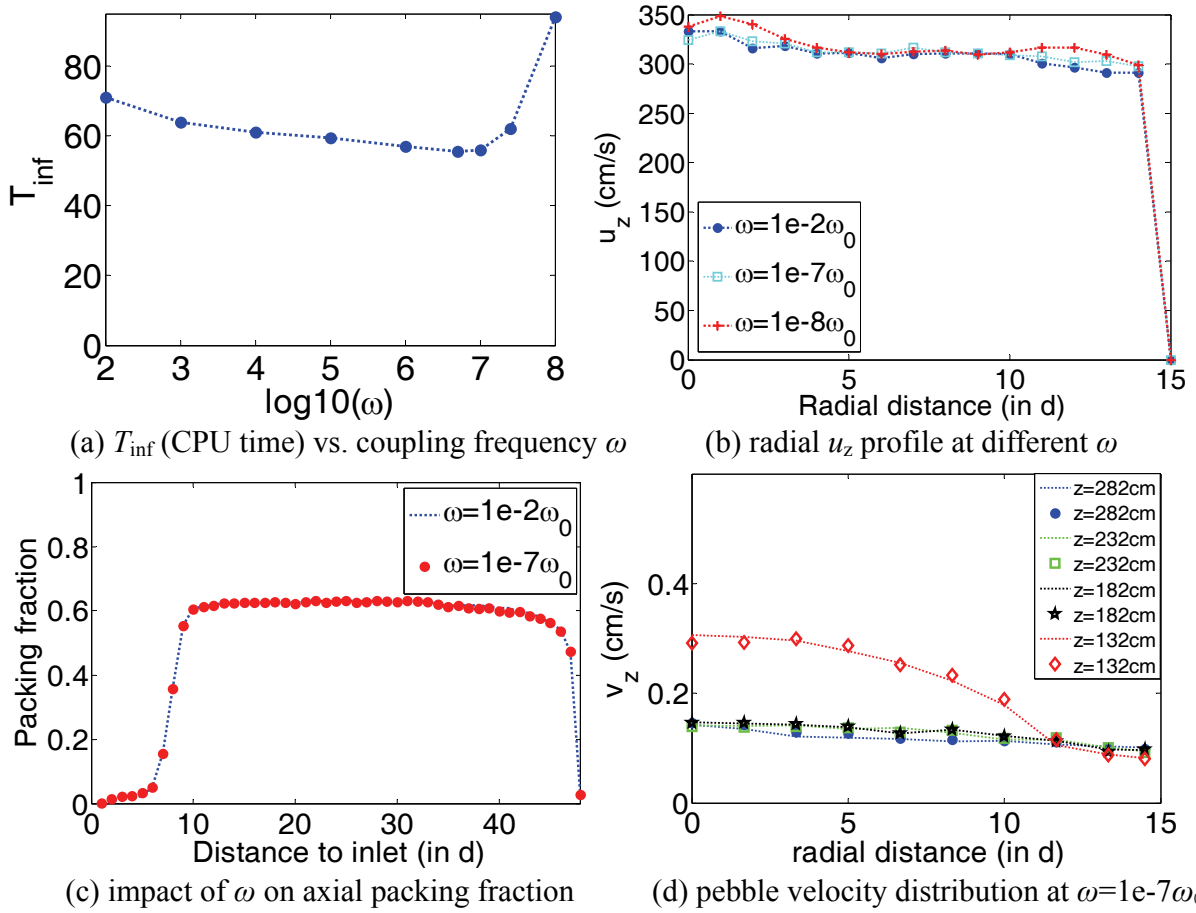

(a) T_{inf} (CPU time) vs. coupling frequency ω (b) radial u_z profile at different ω

(c) impact of ω on axial packing fraction (d) pebble velocity distribution at ω=1e-7ω_0

Figure 7. Impact of coupling frequency ω on computation efficiency and accuracy

In order to investigate the impact of ω on the computation accuracy, the radial distribution of the u_z profile averaged over the cylindrical core region is studied and shown in Fig. 7b. From the figure, we can see that for ω>1e-7ω_0, the radial profile of averaged u_z is very close to the original ω=1e-2ω_0 result with full 3D simulation (r_P≥0.980). Larger error is observed for smaller ω value, and significant deviation is exhibited from ω=1e-8ω_0 (r_P=0.932), due to the lower packing fraction calculated in the center region for very small ω value. By trading off between the efficiency and accuracy, it is suggested that ω=1e-7ω_0~1e-6ω_0 (1 CFD calculation per 10~100seconds) is the optimal coupling frequency range for the HTR application.

Although there is minor deviation in the radial distribution of u_z, which is due to the corresponding radial packing fraction differences caused by loosened coupling, the axial profiles

of pebble packing fraction do not show much difference (r_P=0.992), as shown in Fig. 7c. Since the axial pebble packing fraction distribution is the only pebble flow factor that affects the axial profile of averaged u_z, which is based on the continuity equation, it can be inferred that the consequent u_z profile will not have any appreciable difference.

Since the pebble velocity distribution also influences the thermal-hydraulic calculation, the impact of coupling frequency onto the pebble velocity distribution is also necessary to investigate. In Fig. 7d, the radial pebble velocity profiles at different heights at steady state are shown. The dotted lines correspond with the results of the original ω=1e-2ω_0 frequency and the marks correspond with the ω=1e-7ω_0 frequency. From the figure we can see that at ω=1e-7ω_0, the radial profiles of pebble velocity still well keep track with the original coupling frequency results (with the average $r_P \geq 0.98$), except for the region near the inlet (z=282cm) and the outlet (z=132cm), where the spatial variation of the flow is more significant (or the flow is developing) compared with the middle core region.

Based on the above results shown in Fig. 7, it can be concluded that the optimal coupling frequency with best balance between efficiency and accuracy lies within the region ω=1e-7ω_0~1e-6ω_0.

4. CONCLUSION

In this work, two acceleration strategies are proposed for the coupled DEM-CFD approach in PBR applications. First, a simplified 3D-DEM/2D-CFD approach is proposed based on the axial symmetry of PBRs. Compared to the full 3D-DEM/3D-CFD simulation, the simplified approach can save more than 70% of CPU time at the original coupling frequency of 1e-2ω_0 for the HTR-10 geometry simulation. Due to the geometry symmetry, tangential components and variations of fluid velocity and other flow quantities are small throughout the core region, which brings in insignificant accuracy loss during the averaging. High similarities with the 3D simulation in the cylindrical region are observed for packing statistics, fluid velocity distribution, and pressure drop. Near the inlet/outlet region, due to low and uneven packing fraction, the tangential variation and fluid-pebble interaction is more significant, which results in slight discrepancies between the 3D CFD and the simplified approach results. The dimension reduction

barely alters the steady system constant $T_{cyl,}$ although it reduces the computation efficiency by reducing the transient system constant T_{inf} from more than ten days in the full 3D computation to three days in the simplified calculation.

The second strategy is to reduce the coupling frequency between CFD and DEM solvers. The impact of the coupling frequency on the calculation efficiency and accuracy is investigated. The results show that the decrease of the coupling frequency barely changes the steady state system time constant T_{cyl}, but has a significant impact on the transient system constant T_{inf} when expressed in CPU time. The optimal frequency range ω=1e-7ω_0~1e-6ω_0 is observed considering both the efficiency and radial distribution of vertical coolant velocity profile, which can enhance the computation efficiency by 25% compared with the original coupling frequency of 1e-2ω_0. For an even lower coupling frequency, both the accuracy and efficiency will be compromised. The accuracy impact of the coupling frequency on the axial packing profile of pebbles is not appreciable.

Since the dimension reduction strategy has already been successfully demonstrated in other faster moving particle-fluid systems, such as a fluidized bed, this acceleration technique could also be extended from steady state analysis to accidental transient scenarios, such as earthquakes and loss of coolant accidents, where the time variations of both fluid and pebbles are fast. Due to the greatly enhanced efficiency of the simplified approach, a quick prediction and decision is possible to be made based on the calculation, although the coupling frequency needs to be increased from the optimal value in order to more accurately preserve the temporal variation of flow quantities.

The acceleration of pebble-coolant flow simulations presented in this work enhances the computational efficiency with negligible loss of accuracy, which significantly relieves the computational challenge in PBR modeling and enables the incorporation of other important physics such as thermal and neutronic effects in the future work.

REFERENCES

Auwerda, G.J., Kloosterman, J.L., Lathouwers, D., van der Hagen, T.H.J.J., 2010. Effects of

random pebble distribution on the multiplication factor in HTR pebble bed reactors. Annals of Nuclear Energy 37, 1056-1066.

Cundall, P.A., Strack, O.D.L., 1979. Discrete Numerical Model for Granular Assemblies. Geotechnique 29, 47-65.

Di Felice, R., 1994. The voidage function for fluid-particle interaction systems. International Journal of Multiphase Flow 20, 153-159.

Drew, D.A., 1983. Mathematical modeling of two-phase flow. Annual Review of Fluid Mechanics 15, 261-291.

Drew, D.A., Lahey, R.T.J., 1993. Analytical Modeling of Multiphase Flow, in: Roco, M.C. (Ed.), Particulate Two-Phase Flow. Butterworth-Heinemann, Boston, pp. 509-566.

Ekambara, K., Dhotre, M.T., Joshi, J.B., 2005. CFD simulations of bubble column reactors: 1D, 2D and 3D approach. Chemical Engineering Science 60, 6733-6746.

Enwald, H., Peirano, E., Almstedt, A.E., 1996. Eulerian two-phase flow theory applied to fluidization. International Journal of Multiphase Flow 22, Supplement, 21-66.

Forterre, Y., Pouliquen, O., 2008. Flows of Dense Granular Media. Annual Review of Fluid Mechanics 40, 1-24.

Gao, Z., Shi, L., 2002. Thermal Hydraulic Calculation of the HTR-10 for the Initial and Equilibrium Core. Nuclear Engineering and Design 218, 51-64.

Häne, B.G., Jäger, K., Drexler, H.G., 1993. The Pearson product-moment correlation coefficient is better suited for identification of DNA fingerprint profiles than band matching algorithms. Electrophoresis 14, 967-972.

Hao, C., Li, F., Zhang, H., 2012. The challenges on uncertainty analysis for pebble bed HTGR, PHYSOR 2012-Advances in Reactor Physics, Chicago, IL. La Grange Park, IL: American Nuclear Society, Knoxville, Tennessee, April 15-20, 2012.

Hu, H.H., Patankar, N.A., Zhu, M.Y., 2001. Direct Numerical Simulations of Fluid-Solid Systems Using the Arbitrary Lagrangian-Eulerian Technique. Journal of Computational Physics 169, 427-462.

Ishii, M., 1975. Thermo-Fluid Dynamic Theory of Two-Phase Flow Paris: Eyrolles.

Johnson, K.L., 1985. Contact Mechanics. Cambridge University Press. Cambridge, United Kingdom.

Kafui, K.D., Thorntona, C., Adamsb, M.J., 2002. Discrete particle-continuum fluid modeling of

gas-solid fluidized beds. Chemical Engineering Science 57, 2395-2410.

Li, Y., Ji, W., 2011. Study on Pebble-Fluid Interaction Effect in Pebble Bed Reactors. Trans. Am. Nucl. Soc. 105, 524-525.

Li, Y., Ji, W., 2012. A Collective Dynamics-based Method for Initial Pebble Packing in Pebble Flow Simulation. Nuclear Engineering and Design 250, 229-236.

Li, Y., Ji, W., 2013. Pebble Flow and Coolant Flow Analysis Based on a Fully Coupled Multi-Physics Model. Nuclear Science and Engineering 173, 150-162.

Lim, E.W.C., Wang, C.-H., Yu, A.-B., 2006. Discrete element simulation for pneumatic conveying of granular material. AIChE Journal 52, 496-509.

Lun, C.K.K., 1991. Kinetic theory for granular flow of dense slightly inelastic, slightly rough spheres. Journal of Fluid Mechanics 233, 539-559.

Lun, C.K.K., Savage, S.B., Jeffrey, D.J., Chepurniy, N., 1984. Kinetic theories for granular flow: inelastic particles in Couette flow and slightly inelastic particles in a general flowfield. Journal of Fluid Mechanics 140, 223-256.

Lyngfelt, A., Leckner, B., Mattisson, T., 2001. A fluidized-bed combustion process with inherent CO2 separation application of chemical-looping combustion. Chemical Engineering Science 56, 3101-3113.

Ougouag, A.M., Ortensi, J., Hiruta, H., 2009. Analysis of an Earthquake-Initiated-Transient in a PBR, Proceedings of the International Conference on Mathematics, Computational Methods & Reactor Physics (M&C 2009), Saratoga Springs, New York. La Grange Park, IL: American Nuclear Society, May 3-7, 2009.

Parry, A.J., Millet, O., 2010. Modeling blockage of particles in conduit constrictions: dense granular-suspension flow. Journal of Fluid Engineering 132, 011302.

Reitsma, F., 2012. Reactivity considerations for the on-line refueling of a pebble bed modular reactor-illustrating safety for the most reactive core fuel load. Nuclear Engineering and Design 251, 18-29.

Rodgers, J.L., Nicewander, W.A., 1988. Thirteen Ways to Look at the Correlation Coefficient. The American Statistician 42, 59-66.

Rycroft, C.H., Grest, G.S., Landry, J.W., Bazant, M.Z., 2006. Analysis of granular flow in a pebble-bed nuclear reactor. Physical Review E 74, 021306.

Teuchert, E., Rutten, H.J., 1975. Core Physics and fuel cycles of the pebble bed reactor. Nuclear

Engineering and Design 34, 109-118.

Toit, C.G.d., Rousseaua, P.G., Greyvensteina, G.P., Landmanb, W.A., 2006. A system CFD model of a packed bed high temperature gas-cooled nuclear reactor. International Journal of Thermal Sciences 45, 70-85.

Tsuji, Y., 2007. Multiscale modeling of dense phase gas-particle flow. Chemical Engineering Science 62, 3410-3418.

Verzicco, R., Orlandi, P., 1996. A finite-difference scheme for three-dimensional incompressible flows in cylindrical coordinates. J. Comput. Phys. 123, 402-414.

Xiao, H., Sun, J., 2011. Algorithms in a Robust Hybrid CFD-DEM solver for Particle-laden flows. Communications in Computational Physics 9, 297-323.

Yates, J.G., 1983. Fundamentals of fluidized bed chemical processes. Butterworth Publishers, Stoneham, MA.

Zhu, H.P., Zhou, Z.Y., Yang, R.Y., Yu, A.B., 2007. Discrete particle simulation of particulate systems: Theoretical developments. Chemical Engineering Science 62, 3378-3396.